Author’s response to:
RC#1 and RC#2 from anonymous referees #1 & #2
https://doi.org/10.5194/egusphere-2025-5808-RC1
https://doi.org/10.5194/egusphere-2025-5808-RC2

Jonas Witthuhn[1,2], Hartwig Deneke[1], Andreas Macke[1], Oscar Ritter[1], Jens Redemann[3], Connor J. Flynn[3], Abdulamid A. Fakoya[3], Bradley F. Lamkin[3], Emily D. Lenhardt[3], Logan T. Mitchell[3], Emily K. West[3], David M. Romps[4], Rusen Öktem[4], and Heike Kalesse-Los[2]

[1]Leibniz Institute for Tropospheric Research, Leipzig, Germany
[2]Leipzig Institute for Meteorology, Leipzig University, Leipzig, Germany
[3]School of Meteorology, University of Oklahoma, Norman, OK, USA
[4]Department of Earth and Planetary Science, University of California, Berkeley, CA, USA

Correspondence: jonas.witthuhn@tropos.de

Dear Referee #1 and Referee #2,

Thank you for carefully reading the manuscript and pointing out needs for clarification and recommendations to improve the manuscript. We have revised the manuscript accordingly, below you’ll find the detailed response.

In order to separate the reviewer’s comments and the author’s response, we printed the comments in black and the response in blue. Excerpts of the manuscript with marked changes are pinned directly to the appropriate responses, with the indicated text location (e.g., line number) referring to the manuscript in preprint.

Sincerely, on behalf of all authors

Jonas Witthuhn

Response to RC#1 of Anonymous Referee #1:

General comments

– *To me, the study lacks quantitative information about the effects. Many violin plots are provided visualizing orange vs blue data, but how close or different those are? Are the differences orange-blue statistically significant? For example, L 291 mentions "significant": in which sense significant? Also comparison with other studies: when similarities are mentioned, is it possible to say if they are quantitatively similar? How big effects can be expected?*

* We have revised the discussion section and added quantitative information when possible or applicable from references and from the study dataset. We have added a new figure (Fig.12) to the discussion section which provides the link of absolute change of external variables and enhancement amplitude ϵ and e-folding distance x_e as recommended in the specific comments section. For details please refer to the specific comments section and the marked up document.

– *I would appreciate a better explanation of the analyses of transition signatures with regards to cloud shadow mask/with regards to flow (Sec. 4.1 vs Sec. 4.2).*

* We have revised the introductions and titles of both sections. Please refer also to the changes outlined in the specific comments section.

Sect. 4.1 line 256ff. (*preprint*):

4.1 Signatures analysed with ~~geometrical~~ distance information from COGS

Transition signatures are shown and analysed versus the geometric horizontal distance to the mask edge in Figs. 6, 7, 8, and 9. ~~Observations of GHI are~~ This is achieved using the COGS cloud and shadow masks as 2D information for the calculation of the distance to the nearest cloud and shadow edge (see Sect. 2.2). Therefore, this analysis is tied to the temporal resolution of COGS. At every COGS time step, the GHI observation of PyrNet is supplemented with information on the distance and direction to the nearest cloud and shadow edge.

The GHI observations are then aggregated into distance bins and are shown relative to ~~its~~ their modelled clear sky reference value.

Sect. 4.2 line 328ff. (*preprint*):

4.2 Signatures ~~with~~ analysed with distance relative to flow

Focusing ~~with~~ in greater detail on the radiation enhancement peak close to the cloud shadow, we ~~examined~~ analyse the transition signatures identified by PyrNet ~~in relation to~~ as a function of the distance to the cloud shadow edge~~computed~~, derived from the flow vector. In this part of the analysis, we use only PyrNet measurements, supplemented by flow information. The high temporal resolution enables for a more detailed examination of the signature peaks. Because two-dimensional information is not used in this part of the study, we restricted the analysis to a small area around the transition peak, which is predominantly affected by the cloud whose shadow has just passed over the station. The identified transition signatures are fitted to obtain the two parameters ϵ and x_e, which represent the amplitude of the enhancement peak and the e-folding distance, respectively. In a second step, variations in external observed variables are compared with ϵ and x_e to assess their statistical feature importance, working towards a parametrisation of cloud shadow transition signatures.

Specific comments

– *L 20-21: Plant photosynthesis and feedbacks belong to the previous sentence about land-atmosphere interactions, and photovoltaic power generation is more of an engineering application.*

* We agree and reorganized the paragraph to separate these sub-sentences.

Sect. 1 line 18ff. (*preprint*):

This variability is of scientific interest because it impacts the coupled atmosphere-land system, including the energy balance and the water cycle (Vilà-Guerau De Arellano et al., 2023). ~~In addition, it influences the output and stability of photovoltaic (PV) power generation (e.g., Barry et al., 2020; Kreuwel et al., 2021; Omoyele et al., 2024).~~ It affects plant photosynthesis (Durand et al., 2021; Darko et al., 2023), ~~and even~~ as well as the feedback mechanisms ~~involved in~~ that govern cloud formation and organisation (Jakub and Mayer, 2017). ~~The mentioned~~ These processes are sensitive not only to the total ~~solar energy received~~ amount of incoming solar energy, but also to its spatial and temporal distribution, which is also of particular interest from an engineering standpoint for the performance and stability of photovoltaic (PV) power generation (e.g., Barry et al., 2020; Kreuwel et al., 2021; Omoyele et al., 2024). The scales of this variability range from seconds and metres to hours and kilometres (e.g., Madhavan et al., 2017; Schroedter-Homscheidt et al., 2020; Mol et al., 2024).

– *L 46: I would remove "Building on this network", it does not anything to the sentence if the same data set was used.*

* Agreed and deleted it.

– *L 88: "high concentrations of aerosols from the atmospheric boundary layer": change "from" to "in"*

* Yes we changed it.

– *L 95-96: I do not understand why "however" is used, and why not just report cloud shadow speeds, their direction and cloud cover in one sentence.*

* "However" is used to emphasize a bit, that despite a similar weather pattern during the days of interest, there is some variation in wind speed and direction. But we agree that it is not needed here and simply removed "However,".

– *L 105-106: these instruments, data from which is not used in this study, why they need to be mentioned? instead you could give a bit more information including producers and precision of the instruments that were used for the purposes of this study.*

* We felt that if we opt to not mention the extra pyranometers on a tilted plane here, the readers going to ask the question of their purpose. We agree, that this shouldn't be to extensive as they are not used in the end. To address this, we opt to shorten this statement instead of removing it completely as follows:

Sect. 2.1 line 104ff. (*preprint*):

... At the 30 stations with two pyranometers, solar irradiance from a tilted plane is measured along the GHI measurement (see Fig. 1 (a))~~. Data from the pyranometers on the tilted plane are intended for studies focused on global-to-diffuse irradiance conversion or photovoltaic power production, which is beyond the scope of this current study.~~, but not used in this study.
~~PyrNet photoelectric pyranometers~~ The Eko Instruments ML-020VM pyranometers are of photoelectric type which have a spectral range from 400 to 1100 nm and response time (to reach 95 % of final output value following a sudden change in irradiance) of about 10 ms~~, and are therefore~~. Due to this response time they are perfect for fast sampling ~~to analyse~~ of rapid changes of GHI (Madhavan et al., 2016) ...

The paragraph continues about quality assurance. The next paragraph in this section describes expected uncertainty of GHI measurements an calibration with the used ML-020VM Pyranometers from Eko Instruments in the PyrNet, referencing Madhavan et al. (2016) again, which describes these uncertainties in detail. We chose to not apply changes to this descriptions.

– *Caption to Fig. 4 "shadow chord lengths represent arbitrary cross-sections of the shadow shape due to the stationary nature of the measurements" – this point is not completely clear to me.*

* We acknowledge that this sentence may not be clear and have reworded this part.

Fig. 4 caption (*preprint*):

... The measure D represents a linear cloud size representation, which differs from the cloud shadow chord length recorded by PyrNet for two key reasons. Firstly, the relationship between shadow size and actual cloud size varies based on sun elevation and cloud height. Secondly, because the ~~measured~~ measurements are taken at fixed positions, the recorded shadow chord lengths ~~represent~~ capture only arbitrary cross-sections of the ~~shadow shape due to~~ respective cloud shadows passing the ~~stationary nature of the measurements~~stations...

– *L 195: "-60m towards shadow and 600m towards ..." It is confusing when speaking about time series in the previous sentence, one uses length as limits. Can you explain better, how you come to these limits?*

* Those limits where arbitrarily chosen to by inspecting the data and find a reasonable data segment size per identified peak, which include the drop to the core shadow and as much unshaded samples for further analyses. We rephrased this paragraph for clarification.

Sect. 3.1 line 193ff. (*preprint*):

Using the SciPy algorithm *find_peaks*, we identified the enhancement peak close to the shadow edge. Thereafter, ~~using~~ employing the flow vector of the cloud field (Sect. 2.2), the time series ~~snippets were limited to -60~~are converted into distance series along the flow direction, centred on the detected peaks. For each of these peaks, a data segment is extracted that extends 60 m towards ~~shadow~~ the cloud shadow from the peak location and 600 m towards the ~~cloud shadow gap relative to the flow from the peak location. The lower limit was chosen to ensure~~ unshaded side of the enhancement peak. These bounds are chosen somewhat arbitrarily based on manual inspection: the first bound is set such that the GHI values ~~drop below the clear sky in the shadow part~~ fall below the clear-sky level within the shadowed part of the segment, while the ~~upper limit ensures that most time series snippets have already encountered another shadow values in the selected days~~second bound is selected where most segments have already intersected another cloud shadow. As a last step, we filtered out the snipped time series that already encountered another shadow within 300 m from the peak, to ensure a relatively undisturbed signature by nearby cloud mechanisms (except *side-escape*).

– *Fig 5, y-axis: "normalized irradiance" – is not it transmittance? also T is used. I think, Lennard-Jones in the caption should be changed to Buckingham (quite innovative use of potential functions, I found it amusing). I also suggest to clarify definition of epsilon; current is ϵ = Tpeak/clearsky (%) but from the figure it looks like CE in % should be simply (Tpeak-1)*100?*

* This is true and thank you for spotting our oversight. The caption is correct which states ϵ is the cloud enhancement in %. The definition of ϵ in Fig. 5 is incorrect. The correct one, as you pointed out, is $\epsilon = 100 * (T_{\mathrm{peak}} - \mathrm{clearsky}) =$

$100 * (T_{\text{peak}} - 1)$. We have changed Fig. (5) accordingly and added the definition as a new equation in the text.

Sect. 3.2 line 215ff. (*preprint*):

The original potential function is modified in the way that ϵ describes the magnitude of the peak of the transition signature in percent versus clear sky ~~; therefore~~ by applying an offset of 1~~is applied.~~ .

$\epsilon = 100 * (T_{\text{peak}} - 1)$

- *L 225: could authors show an example of fitting in Fig. 5?*

* As this figure is just a hand-drawn sketch to point out the important variables and give an impression how Eq. (2) looks, an example fit would not be possible here. An example fit of Eq. (2) is shown in Fig. (10) instead. We have added a sentence referencing Fig. (10) here.

Sect. 3.2 line 225 (*preprint*):

From the results of the fit we calculate x_e from Eq. (2). An example fit is shown in Fig. (10).

– *Intro to Section 4: side-escape, forward-escape and albedo-enhancement mechanisms: would be good to have a short discussion how those mechanisms could be separated from each other or how they manifest themselves in the current framework. It would also benefit a reader, if the authors could name there all the cloud variables to be considered.*

* We did a rework of the intro to section 4 with respect to this comment.

Sect. 4 line 233ff. (*preprint*):

During a cloud gap, that is, in between two cloud shading events, the GHI is strongly enhanced compared to clear sky as shown in Fig. 3, where noon GHI values are about 20 % larger in cloud gaps than the reference clear sky values. ~~Radiation enhancement is possible, due to enhanced diffuse irradiation caused by reflection on nearby cloud edges, or in thin cloud situations with cloud optical depth (COD) lower than 10 due to enhanced direct irradiance by strong forward scattering properties of cloud droplets. In cumulus cloud situations, the first effect may be dominant, as these clouds quickly grow and become thicker with COD larger than 10.In Fig. 3, cumulus clouds~~ Cumulus clouds appear around 16:00 UTC and [...] single cloud shadow transitions.

Radiation enhancement can occur as a result of increased diffuse irradiance produced by reflections at nearby cloud edges (*side-escape*). Consequently, the *side-escape* mechanism is likely the dominant factor controlling the e-folding distance x_e on the bright side of the transition signature function (Eq. (2)). For optically thin clouds with cloud optical depth (COD) below 10, radiation enhancement may also arise in the direct irradiance due to the pronounced forward-scattering characteristics of cloud droplets (*forward-escape*). The *forward-escape* mechanism likewise affects the e-folding distance by shaping the sharpness of the enhancement peak and strongly depends on the droplet scattering phase function, which is in turn governed by their effective radius. We do not account for phase (ice versus liquid) in this work, as we concentrate on shallow cumulus clouds with negligible ice content. Both *forward-* and *side-escape* mechanisms modify the bright side of the transition signature and are therefore expected to exert the strongest influence within the scope of our investigation. As shallow cumulus clouds rapidly deepen and attain COD values exceeding 10, the *side-escape* mechanism likely shows the strongest influence. The two mechanisms, *albedo-enhancement* and *downward-escape*, tend to increase diffuse irradiance within the shadow of the cloud. As a result, radiation levels may exceed clear-sky values near the cloud edge due to these processes, and the enhancement peak is extended further into the shadow region. The key parameters are the effective cloud droplet radius and COD for *downward-escape* and surface albedo for *albedo-enhancement*.

To study cloud shadow transitions in more detail [...] the cloud whose shadow recently moved past the station.

To characterise specific cloud properties, we rely on the following externally observed variables: CBH, geometrical cloud depth, and shadow chord length, which constrain the geometrical extent of the cloud; COD and droplet effective radius, which represent the optical characteristics of the clouds. Additionally, the sunlight chord length and the cloud fraction of opaque clouds indicate how separated or clustered individual clouds are. The sun's position and the atmospheric water vapour content are also taken into account to better constrain each individual situation.

– *Caption to Fig. 6: "distance to the respective cloud (orange) or shadow (blue) mask edge". Only shadow is mentioned in x-axis label. Also probably I missed it, but how were the masks (distance) collocated with GHI analyses (time series)?*

* We corrected the x-axis label of Fig. 6 and added a reference to Sect. 2.2 to the intro of Sect. 4.1.

Sect. 4.1 line 257ff. (*preprint*):

Transition signatures are shown versus the geometric horizontal distance to the mask edge in Figs. 6,7,8, and 9. This is achieved using the COGS cloud and shadow masks as 2D information for the calculation of the distance to the nearest cloud and shadow edge (see Sect. 2.2). Observations of GHI are shown relative to its modelled clear sky reference value.

– *Section 4.1 title does not really say anything; cloud vs shadow mask?*

* We agree and updated both Sect. 4.1 and 4.2 titles in this regard.

Sect. 4.1 line 256. (*preprint*):

4.3 Signatures analysed with ~~geometrical~~ distance information from COGS

Sect. 4.2 line 328. (*preprint*):

4.4 Signatures analysed with distance relative to flow

– *L 271-272: reference is needed about 200 m distance*

* We have revised this paragraph because it focuses on interpreting the figure, rather than on a discussion grounded in references.

Sect. 4.1 line 268ff. (*preprint*):

This radiation enhancement peaks closest to the cloud shadow, but is already noticeable at roughly 1 km from the cloud shadow, indicating significant 3D-radiative effects, ~~referred to as~~ due to the *side-escape* mechanism (e.g., Mol and Van Heerwaarden, 2025). Moreover, the most pronounced enhancement is ~~observed within~~ found in the -100 to -200 m bin, which ~~could be attributed to several factors. Small openings in the clouds, particularly at their edges, cause radiation enhancement up to 200 within the cloud shadow, as identified by the COGS mask . Additionally,~~ may stem from small gaps in the cloud cover, especially near cloud edges, that are not captured by the cloud mask because of the COGS resolution~~may lead to partial bin filling by clouds, resulting in them being marked as clouds in the mask. Cloud~~ . In addition, cloud edges are optically thin, ~~related to the path of direct sunlight, leading to another 3D-effect, termed~~ so the *forward-escape* ~~, which~~ mechanism enhances radiation through ~~notable~~ pronounced forward scattering in ~~the cloud edge region~~these edge regions.

– *L 287: "is more pronounced on the sunlit side of the cloud, also depending on the cloud depth". I would appreciate illustration of sunlit vs dark side somewhere in the figures. Then about this effect: how strong effect was found in this study?*

* We have added a sketch to Fig. 7 to illustrate the dark and lit side of a cloud. The enhancement comparing the transition on the lit and dark side of the cloud was pretty significant in Mol and Van Heerwaarden (2025). In section 5.5. they showed cumulonimbus clouds and they found 5 to 10 times stronger enhancement even for clouds of 500 m geometric cloud depth, which is comparable to the cloud heights in the S2VSR field campaign.

Sect. 4.1.1 line 284ff. (*preprint*):
Mol and Van Heerwaarden (2025) studied radiation enhancement for shallow cumulus clouds and found that the peak enhancement varies significantly with sun-cloud geometry. Their simulations focused on the *side-escape* mechanism, setting the surface albedo to zero. They found that the radiation enhancement peak is more pronounced on the sunlit side of the cloud ~~, also depending on the~~ and that this effect also depends on cloud depth. ~~With reduced cloud depth ,~~ As the cloud depth decreases, the enhancement in radiation becomes weaker, though the ~~radiation enhancement diminishes but the~~ sunlit side ~~remains to be markedly~~ still remains significantly brighter than the shaded side. For instance, they reported roughly a 5 to 10 times stronger enhancement on the sunlit side of cumulus clouds with a depth of 500 m. In our case, the mean cloud depth is approximately 300 m. However, in our observations shown in Fig. 7 panel (a), these findings could not be replicated.

– *L303: "shadow irradiance near the sunlit side showed a slight increase, highlighting the notable influence of the albedo-enhancement" - I do not see this from the figure. What also puzzles me is that optically thickest clouds (b) show the same measured-to clear sky GHI ratio as all cases (a), about 40%. why is that? I would expect thickest clouds should have lower transmittance.*

* As we agree, that the absolute differences of values shown in the -200m to 0m range bin are small, there is a notable difference between the ratio values of dark and lit side in panel (b) compared to panel (a), which is what this sentence refers to. To your seconds hesitation: Yes, the differences are very small as panel (a) shows all situation including COD>15, while panel (b) only the isolated COD>15 cases. A better comparison is presented later in Fig. 8 panel(b), where cloud shadows in COD<15 cases show ratios slightly above 0.4 and cases with COD>15 below 0.4. The absolute difference is small, as the total variation of COD is small.

– *L 337: "radiation enhancement, approximately 2% above the existing enhancement level near the shadow's edge" – enhancement over enhancement level is quite confusing.*

* We have rephrased this sentence.

Sect. 4.2.1 line 337ff. (*preprint*):

A ~~sharp rise in radiation enhancement, approximately~~ pronounced increase in GHI can be observed at the edge of the shadow, about 2 % ~~above the existing enhancement levelnear the shadow's edge, is evident~~higher than the prevailing enhancement level.

– *About x_e and epsilon: I think there is not much information about how much these vary, but results of correlation with different variables. It would be interesting to have these linear correlations visualized in the appendix.*

* We agree and have added the new Fig. 12 to the manuscript. We opt to add it in the main section and not to the appendix as we have referenced it in the discussion section 4.2.2 several times. Please refer to the marked up document for details.

New figure 12:

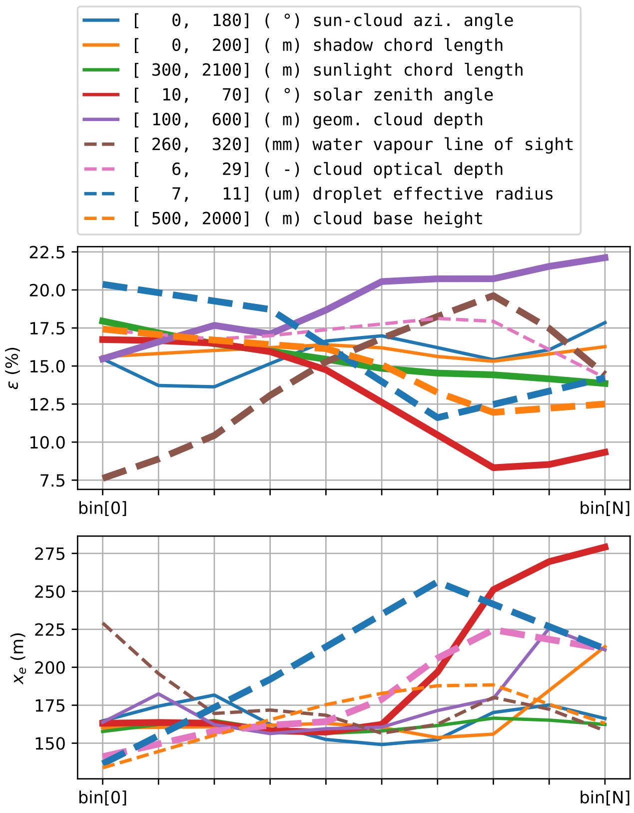

Figure 12. External features in comparison to ϵ and x_e, shown in a standardized binned representation. The legend of the figure indicates the range and units of the features. Lines are drawn with increased thickness if the linear correlation with ϵ and x_e exceeds 0.75.

– *Fig. 11: when feature importance is discussed, what method was used? Is it machine learning based? Which model? It would be good to add this information in Methods.*

* We agree and have added a short sub section in the method part of the manuscript.

New section 3.3:

3.3 Feature importance analysis

We analyse the importance of externally measured variables for the derived ϵ and x_e parameters (see Sect. 3.2). As an initial step, we divided the data into several bins for three different external variables and applied the Virtanen et al. (2020) *SelectKBest* feature selection algorithm. Because our data set is relatively small compared to the large number of external variables, we constrained each feature-selection run to three variables at a time, each split into three bins. We then evaluated all possible combinations of three variables drawn from the entire set of external measurements. The choice of triplets is somewhat arbitrary, but provides a compromise between exploring a wide range of combinations and maintaining sufficient statistical robustness.

The *SelectKBest* method returns univariate F-test scores that quantify the linear dependence between each external variable and the target for a given triplet of variables. We consider scores larger than 0.3 to be significant. For each variable, we record how often it achieved a significant score in all combinations in which it appears. These frequencies are finally expressed as a percentage of significant occurrences per combination and are reported in Sect. 4.2.2. This metric indicates which variables are most suitable for parametrisation when the model is restricted to three variables. The objective is to demonstrate a systematic approach to constructing a parametrisation of transition signatures.

– *Fig. 11: It is interesting that epsilon and x_e show correlations of opposite sign with the same variable (e.g., solar zenith angle, droplet effective radius). Since both epsilon and x_e characterize the strength of CE, is it possible to make some kind of estimate of 'best' combinations? Are there optimal combinations of variables?*

* Yes, it is interesting, but not unexpected. ϵ represents the (relative) peak amplitude versus clear sky, the strength of the peak, so to speak. x_e, on the other hand, characterizes how gradually the enhancement tapers off with distance from the cloud-shadow edge, specifically the point where the peak strength drops below $1/e$ of its maximum value. Since x_e is defined relative to the peak strength, it can certainly occur that x_e increases while ϵ decreases. Regarding optimal combinations, we refrain from proposing a single "best" set of only a few external variables, since it has shown that the optimal choices for peak amplitude and e-folding distance differ substantially. This is because both geometrical and microphysical properties of the current cloud conditions must be taken into account. This issue is discussed at the end of Section 4.2.2 and in more detail in the conclusions in Section 5.

Sect. 4.2.2 line 386ff. (*preprint*):

Finally, we can summarise that to parametrise the transition signature of radiation enhancement, one needs to consider information from both geometrical and microphysical properties of the present cloud situation. If one had to choose a limited set of external variables to describe transition signatures for shallow cumulus clouds, one would start with the variables of highest significance shown in Fig. 11. The size of the cloud gap, the azimuth angle of the sun to the cloud, and the CBH are the most significant features regarding the peak enhancement amplitude. The droplet effective radius, solar zenith angle, and COD, on the other hand, are significant to describe the sharpness of the enhancement peak.

Response to RC#2 of Anonymous Referee #2:

So I don't have so much to add, as I concur with many comments included in the first review; in particular, some results, as provided in figures 6-9 could be explained a little more clearly and/or more quantitatively. Anyway, I think this is quite a pioneering work that can be a first step for further analysis of the same data set, which could be devoted to better explain causal relationships between the already identified features and the measured radiative effects.

Thank you for the motivating words towards further analysis on the topic. We definitely plan to continue in the future. Please refer to the answers to comments from the first review in the previous sections of this authors response.

Technical details

– *Figure 1. Panel (b) shows so many things. I would suggest using this panel to show only the position of PyrNet stations, and reproduce a similar figure as an additional panel of Figure 2, which would contain the transmittance measurements, the cloud mask, the cloud shadow and so... This would make much easier the comparison of the (suggested) two panels in Figure 2.*

* We agree and moved panel (b) of Fig. 1 as panel (a) of Fig. 2, which now has two panels. Panel (b) of Fig. 1 now only shows the PyrNet layout during S2VSR.

– *Projected valid area and focus area seem to be separated by 0.005 degrees, not 0.01 as you say in the caption of Fig. 2 and also in line 146. I might be missing something, but this is what it seems to be according with dashed lines in Fig. 2.*

* This is correct, good catch! We have corrected the occurrences in the text.

– *Figure 3 caption. Authors say that the blue line is "the mean of all observations" which is not clear to me. "All" means observations in 1h time interval? Or a running mean?*

* We have clarified the figure caption.

Fig. 3 caption (*preprint*):
Observed GHI distributions from PyrNet at 13 June 2023 in hourly bins. The distributions as violin plot indicating extrema values in each bin and are of bi-modal shape in the presence of clouds (cloud shadow and shadow gap with enhanced radiation). In addition, the GHI mean ~~of~~ over all ~~observations~~ PyrNet stations in 1 min resolution (blue line) and the calculated enhancement level in cloud shadow gaps (black), and the clear sky reference modelled by the Solis simple model (orange) are shown.

– *The definition of epsilon (ϵ) is not clear to me, and actually, is provided only in Figure 5 and its caption. If T is already a kind of normalized irradiance, why do you need to divide it again by clearsky? Or is ϵ only the same as T but in %?*

* Yes, this was an oversight. The definition provided in the sketch (Fig. 5) is not correct. The definition of ϵ is indeed just the cloud enhancement in %. So the correct definition is $\epsilon = 100 * (T_{\mathrm{peak}} - \mathrm{clearsky}) = 100 * (T_{\mathrm{peak}} - 1)$. We changed

Fig (5) accordingly and added the definition of ϵ as a new equation to the text.

Sect. 3.2 line 215ff. (*preprint*):

The original potential function is modified in the way that ϵ describes the magnitude of the peak of the transition signature in percent versus clear sky ~~; therefore~~ by applying an offset of 1~~is applied.~~ .

$\epsilon = 100 * (T_{\text{peak}} - 1)$

– *In Eq (4) and Eq (5) you use the expression "exp(1)". I understand that this results in the Euler number (e), so why don't you write simply "e"?*

* Yes e and $\exp(1)$ where inconsistently used. We have now changed all appearances of $\exp(1)$ to e.

References

Barry, J., Böttcher, D., Pfeilsticker, K., Herman-Czezuch, A., Kimiaie, N., Meilinger, S., Schirrmeister, C., Deneke, H., Witthuhn, J., and Gödde, F.: Dynamic model of photovoltaic module temperature as a function of atmospheric conditions, Advances in Science and Research, 17, 165–173, https://doi.org/10.5194/asr-17-165-2020, 2020.

Darko, E., Gondor, K. O., Kovács, V., and Janda, T.: Changes in the light environment: Short-term responses of photosynthesis and metabolism in spinach, Physiologia Plantarum, 175, e13 996, https://doi.org/10.1111/ppl.13996, 2023.

Durand, M., Murchie, E. H., Lindfors, A. V., Urban, O., Aphalo, P. J., and Robson, T. M.: Diffuse solar radiation and canopy photosynthesis in a changing environment, Agricultural and Forest Meteorology, 311, 108 684, https://doi.org/10.1016/j.agrformet.2021.108684, 2021.

Jakub, F. and Mayer, B.: The role of 1-D and 3-D radiative heating in the organization of shallow cumulus convection and the formation of cloud streets, Atmospheric Chemistry and Physics, 17, 13 317–13 327, https://doi.org/10.5194/acp-17-13317-2017, 2017.

Kreuwel, F. P., Mol, W. B., Vilà-Guerau De Arellano, J., and Van Heerwaarden, C. C.: Characterizing solar PV grid overvoltages by data blending advanced metering infrastructure with meteorology, Solar Energy, 227, 312–320, https://doi.org/10.1016/j.solener.2021.09.009, 2021.

Madhavan, B. L., Kalisch, J., and Macke, A.: Shortwave surface radiation network for observing small-scale cloud inhomogeneity fields, Atmospheric Measurement Techniques, 9, 1153–1166, https://doi.org/10.5194/amt-9-1153-2016, 2016.

Madhavan, B. L., Deneke, H., Witthuhn, J., and Macke, A.: Multiresolution analysis of the spatiotemporal variability in global radiation observed by a dense network of 99 pyranometers, Atmospheric Chemistry and Physics, 17, 3317–3338, https://doi.org/10.5194/acp-17-3317-2017, 2017.

Mol, W. and Van Heerwaarden, C.: Mechanisms of surface solar irradiance variability under broken clouds, Atmospheric Chemistry and Physics, 25, 4419–4441, https://doi.org/10.5194/acp-25-4419-2025, 2025.

Mol, W., Heusinkveld, B., Mangan, M. R., Hartogensis, O., Veerman, M., and Van Heerwaarden, C.: Observed patterns of surface solar irradiance under cloudy and clear-sky conditions, Quarterly Journal of the Royal Meteorological Society, 150, 2338–2363, https://doi.org/10.1002/qj.4712, 2024.

Omoyele, O., Hoffmann, M., Koivisto, M., Larrañeta, M., Weinand, J. M., Linßen, J., and Stolten, D.: Increasing the resolution of solar and wind time series for energy system modeling: A review, Renewable and Sustainable Energy Reviews, 189, 113 792, https://doi.org/10.1016/j.rser.2023.113792, 2024.

Schroedter-Homscheidt, M., Kosmale, M., and Saint-Drenan, Y.: Classifying direct normal irradiance 1-minute temporal variability from spatial characteristics of geostationary satellite-based cloud observations, Meteorologische Zeitschrift, 29, 131–145, https://doi.org/10.1127/metz/2020/0998, 2020.

Vilà-Guerau De Arellano, J., Hartogensis, O., Benedict, I., De Boer, H., Bosman, P. J. M., Botía, S., Cecchini, M. A., Faassen, K. A. P., González-Armas, R., Van Diepen, K., Heusinkveld, B. G., Janssens, M., Lobos-Roco, F., Luijkx, I. T., Machado, L. A. T., Mangan, M. R., Moene, A. F., Mol, W. B., Van Der Molen, M., Moonen, R., Ouwersloot, H. G., Park, S., Pedruzo-Bagazgoitia, X., Röckmann, T., Adnew, G. A., Ronda, R., Sikma, M., Schulte, R., Van Stratum, B. J. H., Veerman, M. A., Van Zanten, M. C., and Van Heerwaarden, C. C.: Advancing understanding of land–atmosphere interactions by breaking discipline and scale barriers, Annals of the New York Academy of Sciences, 1522, 74–97, https://doi.org/10.1111/nyas.14956, 2023.

Virtanen, P., Gommers, R., Oliphant, T. E., Haberland, M., Reddy, T., Cournapeau, D., Burovski, E., Peterson, P., Weckesser, W., Bright, J., Van Der Walt, S. J., Brett, M., Wilson, J., Millman, K. J., Mayorov, N., Nelson, A. R. J., Jones, E., Kern, R., Larson, E., Carey, C. J., Polat, I., Feng, Y., Moore, E. W., VanderPlas, J., Laxalde, D., Perktold, J., Cimrman, R., Henriksen, I., Quintero, E. A., Harris, C. R., Archibald, A. M., Ribeiro, A. H., Pedregosa, F., Van Mulbregt, P., SciPy 1.0 Contributors, Vijaykumar, A., Bardelli, A. P., Rothberg, A., Hilboll, A., Kloeckner, A., Scopatz, A., Lee, A., Rokem, A., Woods, C. N., Fulton, C., Masson, C., Häggström, C., Fitzgerald, C., Nicholson, D. A., Hagen, D. R., Pasechnik, D. V., Olivetti, E., Martin, E., Wieser, E., Silva, F., Lenders, F., Wilhelm, F., Young, G., Price, G. A., Ingold, G.-L., Allen, G. E., Lee, G. R., Audren, H., Probst, I., Dietrich, J. P., Silterra, J., Webber, J. T., Slavič, J., Nothman, J., Buchner, J., Kulick, J., Schönberger, J. L., De Miranda Cardoso, J. V., Reimer, J., Harrington, J., Rodríguez, J. L. C., Nunez-Iglesias, J., Kuczynski, J., Tritz, K., Thoma, M., Newville, M., Kümmerer, M., Bolingbroke, M., Tartre, M., Pak, M., Smith, N. J., Nowaczyk, N., Shebanov, N., Pavlyk, O., Brodtkorb, P. A., Lee, P., McGibbon, R. T., Feldbauer, R., Lewis, S., Tygier, S., Sievert, S., Vigna, S., Peterson, S., More, S., Pudlik, T., Oshima, T., Pingel, T. J., Robitaille, T. P., Spura, T., Jones, T. R., Cera, T., Leslie, T., Zito, T., Krauss, T., Upadhyay, U., Halchenko, Y. O., and Vázquez-Baeza, Y.: SciPy 1.0: fundamental algorithms for scientific computing in Python, Nature Methods, 17, 261–272, https://doi.org/10.1038/s41592-019-0686-2, 2020.